JACS
JOURNAL OF THE AMERICAN CHEMICAL SOCIETY
Article
Cite This: J. Am. Chem. Soc. XXXX, XXX, XXX−XXX
pubs.acs.org/JACS

Impact of Antifouling PEG Layer on the Performance of Functional Peptides in Regulating Cell Behaviors

Qi Chen,[†] Shan Yu,[‡] Donghui Zhang,[†] Wenjing Zhang,[†] Haodong Zhang,[†] Jingcheng Zou,[†] Zhengwei Mao,[‡] Yuan Yuan,[†] Changyou Gao,[‡] and Runhui Liu*[,†]

[†]State Key Laboratory of Bioreactor Engineering, Key Laboratory for Ultrafine Materials of Ministry of Education, Research Center for Biomedical Materials of Ministry of Education, School of Materials Science and Engineering, East China University of Science and Technology, Shanghai 200237, China

[‡]MOE Key Laboratory of Macromolecular Synthesis and Functionalization, Department of Polymer Science and Engineering, Zhejiang University, Hangzhou 310027, China

Supporting Information

ABSTRACT: Cell adhesive and other functional peptides (such as RGD, KRSR, YIGSR, VAPG, and BMP-2 peptides) are extensively studied and utilized in tissue engineering scaffolds and biomedical devices to modulate cell functions. Though PEG is frequently used as the antifouling layer, it is unclear how it affects the performance of functional peptides. By analyzing the impact of PEG at short (OEG4), medium (OEG8), and long chain length (PEG2K), we reveal that PEG chain length is critical and a medium-length PEG enables functional peptides to display their optimal and genuine functions in cell adhesion, migration, and differentiation by providing excellent antifouling to minimize background noise of unwanted cell adhesion and high enough surface density of functional peptides. Our result provides new avenues for maximizing the genuine functions of peptides. This study also provides a solution to prevent the heterogeneous and even divergent results caused by inappropriate choice of antifouling PEG and provides a general guidance in identifying new functional peptides.

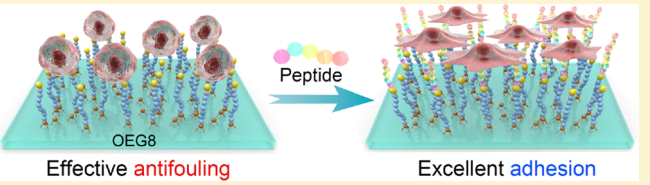

INTRODUCTION

Cell function and cell fate are substantially affected by the interaction between cells and extracellular matrix (ECM) components.[1] Therefore, cell adhesive peptides (CAPs) derived from ECM proteins (such as RGD,[2] KRSR,[3] YIGSR,[4] VAPG[5]) and other functional peptides (such as BMP-2 peptide corresponding to residues 68−87 of bone morphogenetic protein 2 (BMP-2)[6]) are extensively studied and utilized in tissue engineering scaffolds and biomedical devices to facilitate cell adhesion, proliferation, migration, and differentiation.[7−15] At present, only a handful of CAPs are identified, and their functions are not fully understood.[16] To identify new CAPs and explore their genuine interactions with specific cells, it is critical to decouple the nonspecific cell adhesion due to biofouling that is unfortunately universal unless antifouling strategies are applied.[17−22] Polyethylene glycol (PEG) has been extensively used to provide the antifouling layer for covalent immobilization of CAPs.[23−26] Nevertheless, the impact of a PEG antifouling layer on CAPs' function is much less studied.[27,28] The coexistence of CAPs−cell interaction studies using either no antifouling layer at all or PEG at variable chain length causes heterogeneous results that are difficult and even impossible to compare with each other.

To address this overlooked long-lasting and critical problem, we explored the performance of surface-tethered functional peptides, such as CAPs and the BMP-2 peptide, on a layer of PEG at variable chain length, short (tetraethylene glycol, OEG4), medium (octaethylene glycol, OEG8), and long (polyethylene glycol, PEG2K, M_n = 2000 Da). These studies revealed that the chain length of PEG has a substantial impact on the performance of functional peptides by affecting both the antifouling property and then surface density of tethered peptides. An appropriate antifouling PEG at a medium chain length (OEG8) enables both low background and high density of surface-tethered functional peptides to enable optimal performance of peptides for their genuine function in cell adhesion, migration, and differentiation. Inappropriate antifouling PEG with either a short or a long chain, OEG4 or PEG2K, leads to either overestimation or underestimation in cell adhesion and misleading and even wrong conclusions on sophisticated cell migration and differentiation. Our study provides a general guidance in constructing functional surfaces with the appropriate antifouling PEG layer to reveal the genuine performance of functional peptides and to identify new functional peptides with minimum interference from biofouling.

EXPERIMENTAL SECTION

Preparation of Antifouling Surface. Glass coverslips (25.4 × 76.2 mm) were cleaned with ethanol and Milli-Q water in an ultrasonic bath for 15 min individually, dried under a N_2 stream, and then

Received: July 4, 2019

DOI: 10.1021/jacs.9b07105
J. Am. Chem. Soc. XXXX, XXX, XXX−XXX

oxidized and cleaned by a UV-ozone cleaner for 25 min for surface activation. The slide surfaces were incubated with a solution of (3-aminopropyl)triethoxysilane (APTES) in anhydrous toluene at a concentration of 2% (v/v) overnight at room temperature (rt), followed by washing with toluene, ethanol, and Milli-Q water sequentially and drying with a stream of N_2. The APTES-modified glass slides were annealed at 80 °C for 3 h to give the amine-functionalized glass slides. After the amine surface was covered with a 50-well chambered coverslip, an aliquot of 10 μL of bifunctionalized OEG4 Maleimide-OEG4-*N*-hydroxysuccinimide (MAL-OEG4-NHS, 20 mM in DMSO), bifunctionalized OEG8 Maleimide-OEG8-*N*-hydroxysuccinimide (MAL-OEG8-NHS, 20 mM in pH 7.4 phosphate-buffered saline (PBS)), or bifunctionalized PEG2K Maleimide-PEG2K-*N*-hydroxysuccinimide (MAL-PEG2K-NHS, 20 mM in pH 7.4 PBS) was added into each individual well, and then the glass slide was incubated at rt for 2 h. The PEG-modified glass slide was washed with Milli-Q water and dried by a stream of N_2. Each well was then incubated with thioglycerol (100 mM in pH 7.4 PBS) for 2 h, followed by washing with Milli-Q water, ethanol, and Milli-Q water sequentially and drying under a flow of N_2.

Preparation of Peptide/Polymer-Immobilized Surfaces. After the OEG4-, OEG8-, or PEG2K-coated glass slide was covered with a 50-well chambered coverslip, an aliquot of a 10 μL solution of a peptide (KRSR, YIGSR, VAPG, and BMP-2 peptide) at a concentration of 0.25 mg/mL or Nylon3 (β-polypeptide, 60:40 DM:CH) at 2 mg/mL in pH 7.4 PBS (containing 10% (v/v) glycerol) was added to each well, and the slide was incubated at rt overnight. After washing with Milli-Q water and ethanol alternatively for two cycles, an aliquot of 10 μL thioglycerol solution (100 mM in 1× PBS buffer at pH 7.4, supplemented with 10% (v/v) glycerol) was added to each well, and then the slide was incubated for 2 h at rt. The peptides-immobilized surface was then cleaned by Milli-Q water and dried with N_2.

Grafting Density of CAPs Measured by Surface Plasmon Resonance (SPR). SPR analysis was performed on a Biacore T200 spectrometer using custom SPR sensor chips possessing a 15 nm SiO_2 top coating. Phosphate-buffered saline (PBS) was used as the running buffer. All solutions for SPR measurement were freshly prepared and filtered through 0.22 μm filters prior to use. Sensor chips were modified with MAL-OEG4-NHS, MAL-OEG8-NHS, or MAL-PEG2K-NHS using the aforementioned protocol. The baseline was first stabilized by running a PBS buffer at a flow rate of 50 μL/min. Then the flow rate was decreased to 0.25 μL/min, and the flow continued for another 3 min. CAP solution (0.25 mg/mL KRSR, YIGSR, or VAPG) flowed over the OEG/PEG-modified sensing chip for 60 min, followed by flushing the surface with PBS for 10 min to remove nontethered peptide from the surface. The amount of surface-tethered CAPs on different OEG/PEG surfaces was recorded and calculated from the difference in the response unit (ΔRU, 1 RU $\approx$ 1000 pg/cm^2) before and after the surfaces were incubated with the CAPs. The grafting density (pmol/cm^2) of CAP on the surfaces was calculated by the ratio of grafting amount (pg/cm^2) to the M_w of the CAP. Samples were analyzed in triplicates.

Protein Adsorption Test. The OEG4-, OEG8-, PEG2K-, and NH_2-coated glass slides were washed with PBS and then were incubated with BSA-FITC solution (0.5 mg/mL in PBS) in the dark at rt for 30 min. After washing three times with PBS, the fluorescence intensity was quantified using a fluorescent scanner (ImageQuant LAS 4000). The data were analyzed using ImageQuant LAS 4000 Control software.

Cell Attachment Analysis. NIH 3T3 fibroblast cells, endothelial cells (ECs), and smooth muscle cells (SMCs) were cultured in Dulbecco's modified Eagle's medium (DMEM) with or without 10% fetal bovine serum (FBS) (Gibco), 100 U/mL penicillin, 100 μg/mL streptomycin, and 2 mM L-glutamine at 37 °C in a 5% CO_2 environment. MC-3T3-E1 preosteoblast cells were cultured in α-MEM medium. Cells at 80−90 confluency were detached from the Petri dish using 0.25% (w/v) trypsin/EDTA (Gibco), centrifuged to remove the supernatant, and resuspended in culture medium to a final cell concentration of 10^5 cells/mL. An aliquot of 10 μL of this cell suspension was added to each individual well of the peptide-immobilized glass slide. The slide was placed in a Petri dish and incubated at 37 °C for 2 h to allow cell attachment, followed by adding fresh medium into the Petri dish to immerse the entire slide and incubating the slide at 37 °C for 1 day. After excess medium was removed, cells were incubated with a LIVE/DEAD staining solution containing 2 μM calcein AM and 4 μM ethidium homodimer-1 in the dark for 15 min. The fluorescent images were captured under a microscope (Nikon Eclipse Ti-S; Japan) at different locations of each well, and the images were analyzed using ImageJ software.

Cell Migration Analysis. All samples were irradiated under low-density UV light for 30 min for sterilizing. In order to avoid cell−cell interactions, ECs and SMCs were seeded at a low density (5.0×10^3 /cm^2) on the materials, respectively, and incubated overnight to allow cell attachment. Cell migration trajectories were recorded *in situ* under a time-lapse phase-contrast microscope (DMI6000B, Leica) equipped with a transparent chamber to maintain the temperature and humidified atmosphere (37 °C, 5% CO_2). The (x, y) positions at various times of each single cell were exported using ImageJ software with the manual tracking plugins. The starting position of each single cell was automatically normalized to the original position (0, 0). The cell movements were reconstructed from the center positions. The cell migration distance S was calculated by the Chemotaxis Tool (Ibids, Germany) according to the following equation with a 15 min time interval.

$$S = \sum_{i=1}^{t} \sqrt{(x_i - x_{i-1})^2 + (y_i - y_{i-1})^2}$$

At least 50 viable cells were analyzed for each datum. The cell migration rate was obtained from the formula $v = S/t$. The statistical analysis was performed using the t test method, and the significant difference level was set as $p < 0.05$.

Mesenchymal Stem Cell Culture. Mesenchymal stem cells (MSCs) were isolated and collected from 4-week-old Sprague−Dawley (SD) rats. Bone marrow was collected from the femurs and tibiae and then suspended in α-MEM containing 10% FBS (Gibco) for continuous culture in a humidified atmosphere with 5% CO_2 at 37 °C. Nonattached cells were removed by changing the medium after 1 day, and the culture medium was changed every other day. For subculture, cells were passaged at 80−90% confluency and detached by 0.05% trypsin and 0.02% ethylenediaminetetraacetic acid (EDTA). All experiments of MSCs were conducted with cells at passage 3−5.

Alkaline Phosphatase Staining. MSCs were cultured overnight on a peptide-immobilized glass surface using α-MEM medium containing 10% FBS (v/v); then the medium was replaced with α-MEM medium containing 2% FBS (v/v). After incubation for 7 days, the alkaline phosphatase (ALP) activity of MSCs was detected by ALP staining and ALP assay. For ALP staining, the cells were fixed in 4% paraformaldehyde and then stained using the BCIP/NBT alkaline phosphatase color development kit (Beyotime Biotech, C3026, China) according to the manufacturer's protocol. The images were acquired using a microscope. For the ALP assay, cells were lysed using 50 μL of 1% Nonidet P-40 for 1 h followed by mixing (1:1 v/v) with an aliquot of 50 μL of pNPP solution in each individual well of a 96-well plate. After incubation for 60 min, the 96-well plate was shaken for 30 s and the absorbance at 405 nm was measured. The ALP activity was normalized relative to total proteins that were quantified using the BCA Protein assay kit (Beyotime Biotech, P0010, China).

Immunofluorescent Staining. The RUNX2 and OPN assays were conducted after the MSCs were cultured for 7 days and 21 days, respectively. Briefly, cells cultured on the surfaces were fixed in 4% (w/v) paraformaldehyde for 15 min and then permeabilized with 0.4% (v/v) Triton-X 100 (Sigma-Aldrich) in PBS for 5 min. The treated cells were blocked with 3% (w/v) bovine serum albumin (BSA) at 37 °C for 1 h followed by incubation with mouse monoclonal antibody RUNX2 (1:100, Santa Cruz) or mouse monoclonal antibody osteopontin (1:100, Santa Cruz) at 4 °C overnight after blocking with 3% (w/v) BSA. Cells were incubated with Alexa Fluor 488 goat anti-mouse (IgG) (1:200, Abcam) and TRITC-phalloidin (1:200, YEASEN) for F-actin

DOI: 10.1021/jacs.9b07105
J. Am. Chem. Soc. XXXX, XXX, XXX−XXX

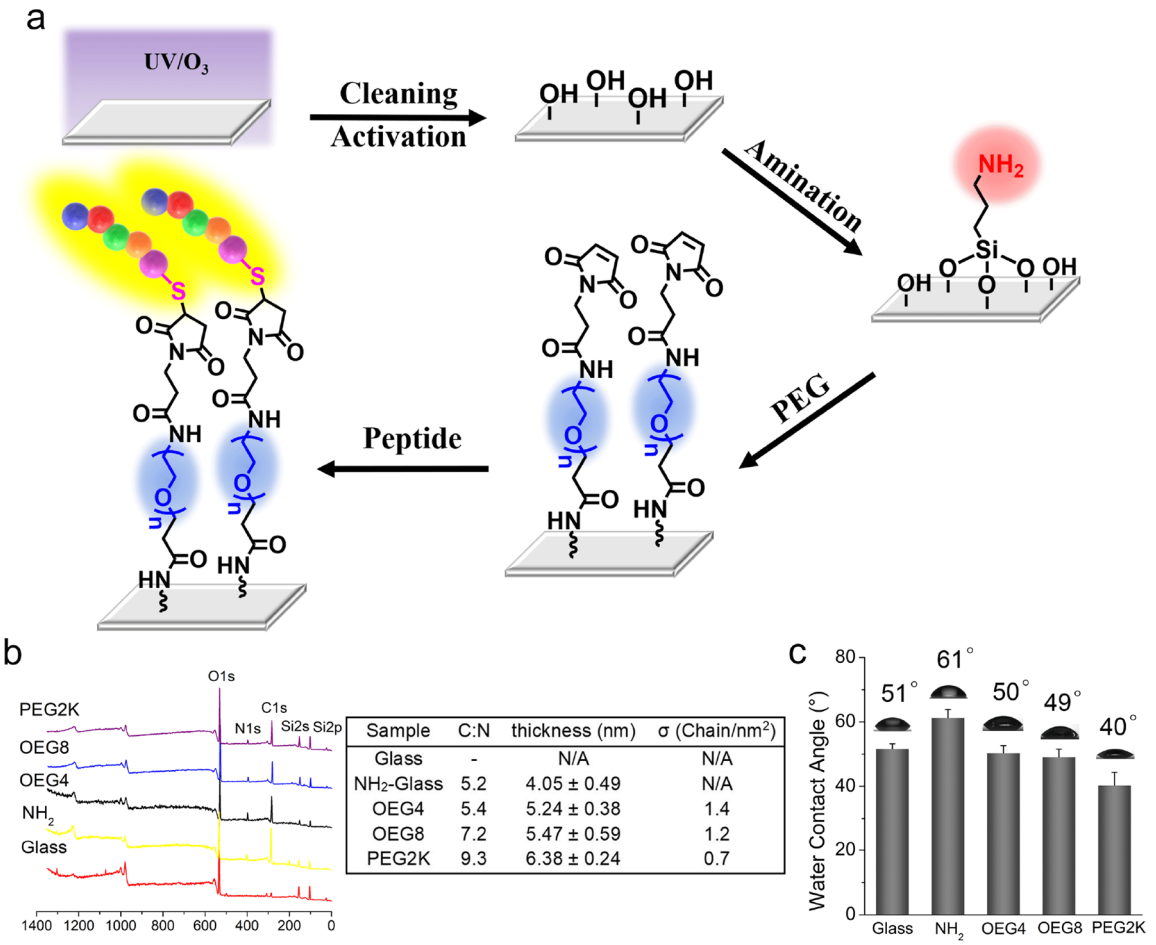

Sample	C:N	thickness (nm)	σ (Chain/nm^2)
Glass	-	N/A	N/A
NH_2-Glass	5.2	4.05 ± 0.49	N/A
OEG4	5.4	5.24 ± 0.38	1.4
OEG8	7.2	5.47 ± 0.59	1.2
PEG2K	9.3	6.38 ± 0.24	0.7

Figure 1. Surface modification and characterization. (a) Glass surface was activated with UV/O_3 followed by amination using (3-aminopropyl)triethoxysilane (APTES) to present glass surface amine groups that react with a heterobifunctional PEG (maleimide-PEG-succinimidyl ester). Then terminal thiol group functionalized peptides were covalently attached to the glass surface by reacting with maleimide groups. (b) PEG modification to the glass surface was confirmed by XPS and ellipsometry characterization, respectively, with a gradually increased carbon to nitrogen ratio (C:N) and surface thickness from NH_2-glass to glass surfaces modified OEG4, OEG8, or PEG2K. σ means the grafting density of the PEG chain on the glass surface.[29] (c) Water contact angle of glass surfaces with or without modification. N/A = not applicable.

staining. The fluorescent images were captured under a microscope (Nikon Eclipse Ti-S; Japan) at different locations in each well, and the fluorescence intensity was quantified using a fluorescent scanner (ImageQuant LAS 4000). The images were analyzed using ImageQuant LAS 4000 Control software.

RESULTS

Glass Surface Modification with CAPs. To study the interactions between cells and CAPs, we tethered CAPs to glass surfaces above a layer of antifouling PEG at variable chain length, OEG4, OEG8, and PEG2K. The bare glass slide was first functionalized with primary amine groups and then modified with the PEG molecules and CAPs sequentially (Figure 1a). After the surface amination and PEG modification step, X-ray photoelectron spectroscopy (XPS) characterization showed apparent C 1s and N 1s peaks, which confirmed a successful surface functionalization with amine groups. A subsequent modification with PEG chains was confirmed by the increased surface thickness and increased C:N element ratio after PEG modification (Figure 1b). The increase and subsequent drop of water contact angle is consistent with the successful sequential surface modification with amine groups and then with PEG chains (Figure 1c). It is noteworthy that we used an easy operating UV/O_3 cleaner for efficient glass surface cleaning and activation as a substitution of "piranha" solution, a mixture of sulfuric acid and hydrogen peroxide, that is very dangerous and must be handled with extra care.

Cell Adhesion Modulated by PEG. We first explored how antifouling PEG modulated the function of cell type specific CAPs (KRSR, YIGSR, and VAPG) that are widely studied and utilized in selective cell adhesion of preosteoblast cells, endothelial cells, and smooth muscle cells, respectively (Figure 2). We found that the short OEG4 as the antifouling layer led to obvious fouling and unwanted background noise of cell adhesion that significantly compromised the cell type specific function of KRSR (preosteoblast vs fibroblast), YIGSR (EC vs SMC), and VAPG (SMC vs EC) on the surfaces (Figure 2a–f). In contrast, PEG2K as the antifouling layer exhibited excellent antifouling property and low background noise of cell adhesion, but results in poor cell adhesion for all three CAPs-modified surfaces (Figure 2a–f). OEG8 as the antifouling layer, however, provides excellent antifouling, low background noise of unwanted cell adhesion, and desired selective cell adhesion for each type of cells using KRSR, YIGSR, and VAPG individually (Figure 2a–f). We explain the observation above using cartoon art (Figure 3a).

The above observation of unwanted background noise of cell adhesion to OEG4-modified surfaces but not to OEG8- and

DOI: 10.1021/jacs.9b07105
J. Am. Chem. Soc. XXXX, XXX, XXX−XXX

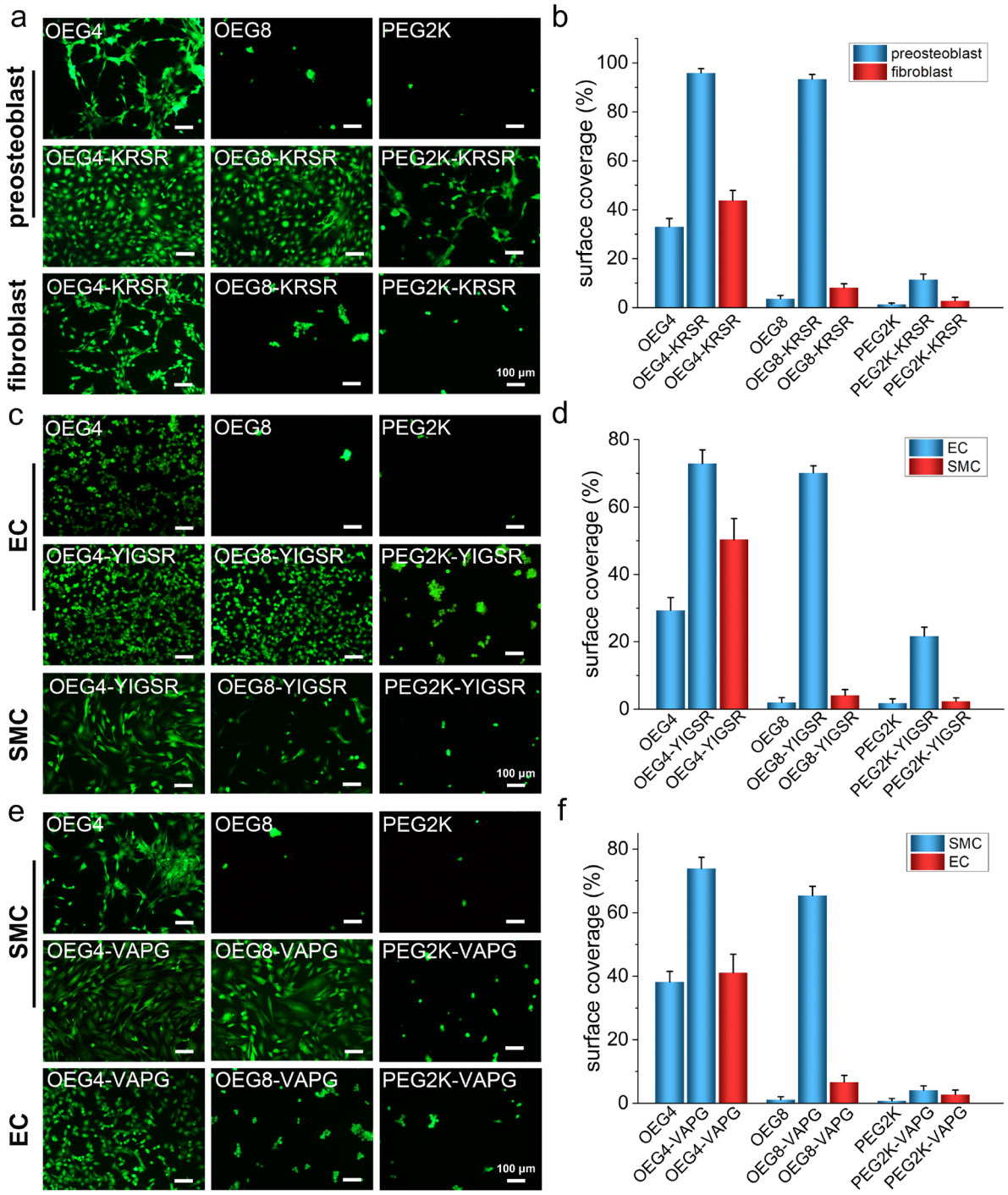

Figure 2. Cell adhesion studies indicate OEG8 as an excellent antifouling layer to demonstrate the genuine and optimal function of cell-selective CAPs. (a, b) Microphotos and surface coverage analysis of MC-3T3 preosteoblast cell and NIH-3T3 fibroblast cell adhesion on OEG4, OEG8, and PEG2K surfaces with and without further modification with preosteoblast-selective KRSR peptide. n = 5 for each group. (c, d) Microphotos and surface coverage analysis of smooth muscle cell (SMC) and endothelial cell (EC) adhesion on OEG4, OEG8, and PEG2K surfaces with and without further modification with EC-selective YIGSR peptide. n = 5 for each group. (e, f) Microphotos and surface coverage analysis of SMC and EC adhesion on OEG4, OEG8, and PEG2K surfaces with and without further modification with SMC-selective VAPG peptide. n = 5 for each group. All above studies were conducted on day 1 post cell seeding in serum-containing environment. Scale bar: 100 μm. All data are presented as means ± SD.

PEG2K-modified surfaces implied that OEG4 is too short to resist unwanted fouling (Figure 3a). This observation is consistent with the protein adsorption result that the OEG4-modified surface resists only 30% protein adsorption, whereas OEG8- and PEG2K-modified surfaces resist 84% and 97% protein adsorption, respectively, relative to protein adsorption on an amine surface (Figure 3b and Figure S1). In addition to antifouling, the choice of PEG molecules (OEG4, OEG8, or PEG2K) can also have a great impact on the density of surface-tethered CAPs (KRSR, YIGSR, or VAPG). We quantified the density of surfaced-tethered CAPs on various antifouling layers using SPR.[30] We found that CAPs (KRSR, YIGSR, and VAPG) all have comparable densities on OEG4 and OEG8 surfaces, which were substantially higher than the peptide density on the

DOI: 10.1021/jacs.9b07105
J. Am. Chem. Soc. XXXX, XXX, XXX−XXX

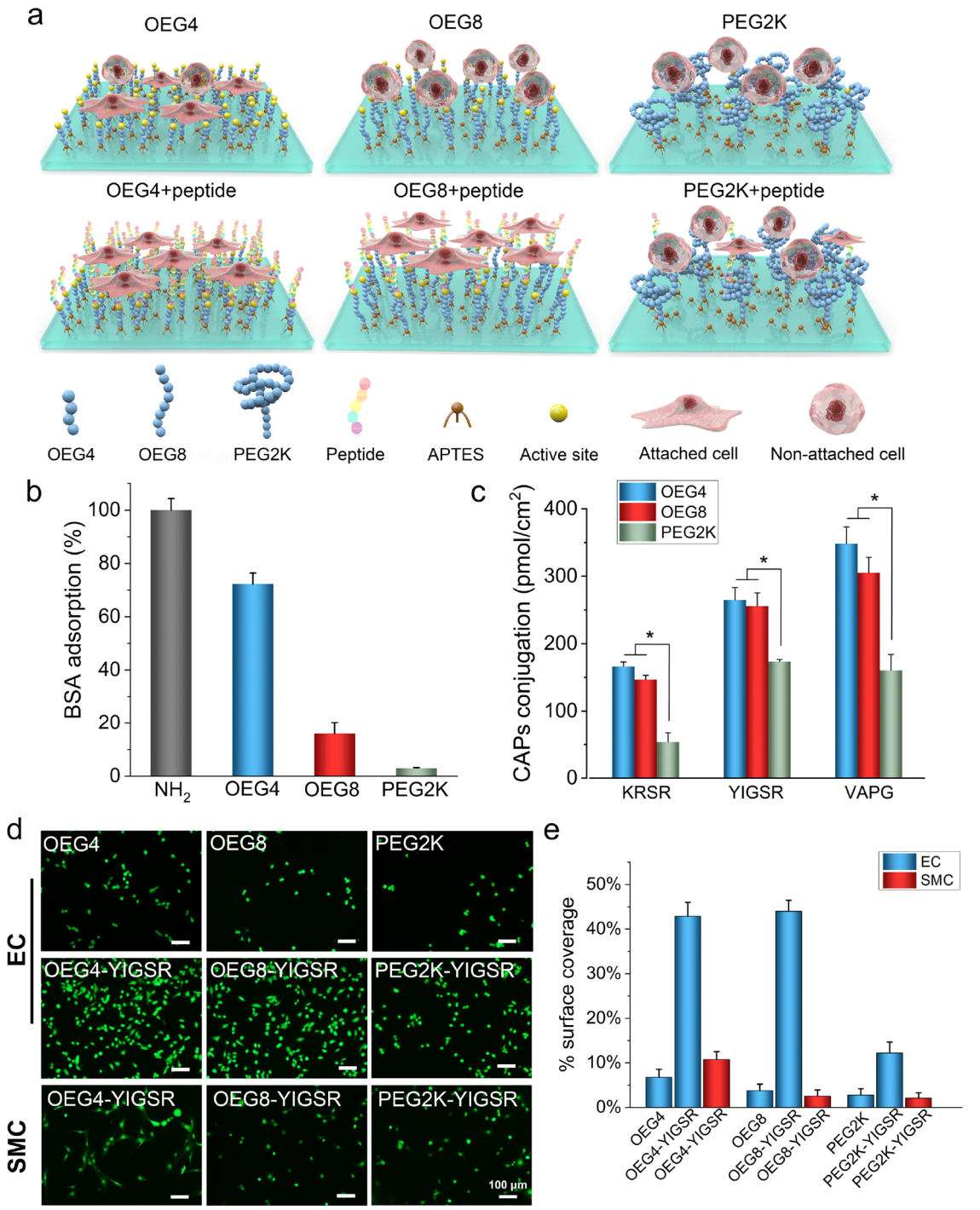

Figure 3. Study on how the antifouling PEG layer affects the genuine function of CAPs. (a) Schematic diagram of cell adhesion on different surfaces. (b) BSA adsorption on various surfaces using the NH_2 surface as 100% BSA adsorption. (c) Density of surface-tethered KRSR, YIGSR, and VAPG on OEG4, OEG8, and PEG2K surfaces measured by SPR. (d, e) Microphotos and surface coverage of EC and SMC after 1 day of incubation on OEG4, OEG8, and PEG2K surfaces with and without further modification with EC-selective YIGSR peptide in the serum-free environment. $n = 5$ for each group.

PEG2K surface (Figure 3c and Figure S2). This result indicated that the favorable cell adhesion onto the OEG8-CAP surface to display the genuine function of CAPs came from both the favorable antifouling property and the high density of surface-tethered CAPs on the OEG8 surface. The low density of CAPs on the PEG2K surface also explained our observation that the PEG2K-CAP surface supported poor cell adhesion in general (Figure 2).

To strengthen our hypothesis and explanation on the observed effect of the PEG antifouling layer, we also examined EC and SMC adhesion on CAPs-modified surfaces (OEG4-YIGSR, OEG8-YIGSR, and PEG2K-YIGSR) in a serum-free environment (Figure 3d,e). This study in a serum-free environment enabled us to abolish the interference of protein fouling on the surfaces and subsequent background noise of unwanted cell adhesion. Under the serum-free condition, we

DOI: 10.1021/jacs.9b07105
J. Am. Chem. Soc. XXXX, XXX, XXX−XXX

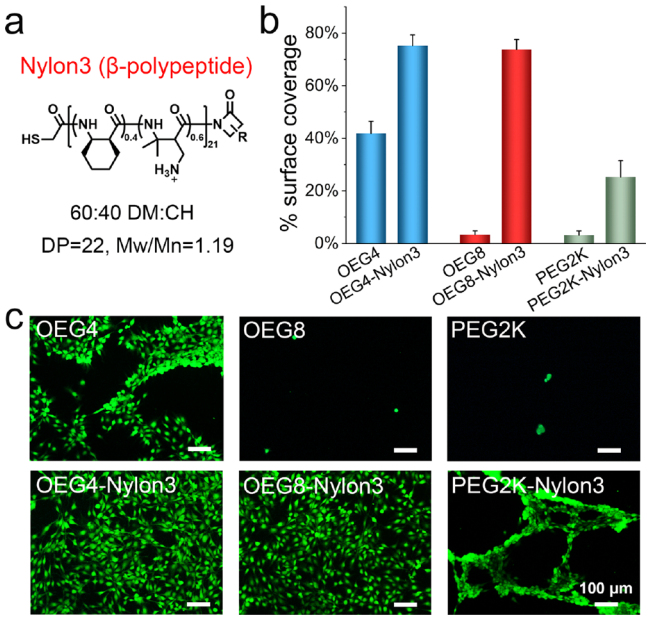

Figure 4. Fibroblast cell adhesion on various antifouling layers modified with Nylon3 polymer. (a) Structure of Nylon3 (β-polypeptide, 60:40 DM:CH). (b) Quantitative analysis on surface coverage by cells on various surfaces 1 day post cell seeding. All data are presented as means ± SD. (c) Micrographs of NIH-3T3 fibroblast cell adhesion on OEG4, OEG8, and PEG2K surfaces with and without further modification of Nylon3 in a serum-containing environment. n = 5 for each group. Scale bar: 100 μm.

observed that cell adhesion was poor even on the OEG4 surface. Moreover, we observed selective and favorable EC adhesion and poor SMC adhesion on OEG4-YIGSR and OEG8-YIGSR surfaces, a desired and genuine performance of EC-selective YIGSR peptide. This result on the OEG4-YIGSR surface is divergent from the poor EC vs SMC selectivity for cell adhesion on the OEG4-YIGSR surface in a serum-containing environment (Figure 2c,d), whereas the protein fouling on OEG4 and OEG4-YIGSR surfaces resulted in high background noise of unwanted SMC adhesion and a loss of the genuine function of EC-selective cell adhesion of the YIGSR peptide. The cell adhesion study in the serum-free environment underpinned our hypothesis and explanation that OEG8 works as an optimal antifouling layer to enable surface-modified CAPs to display their genuine functions by providing both efficient antifouling property and a high density of surface-modified CAPs.

Encouraged by the above study on CAPs, we continued to explore how the antifouling PEG layer effects cell adhesion on the surfaces that were modified with a cell adhesive Nylon3 (β-polypeptide), previously identified as an RGD function mimicking CAP (Figure 4a, GPC and NMR characterization of Nylon3 in Figure S3 and Figure S4, respectively).[29,31] We found that fibroblast cells adhere well to OEG4-Nylon3 and OEG8-Nylon3 surfaces but not to PEG2k-Nylon3 surfaces (Figure 4b,c). This observation indicated similar effects of the antifouling PEG layer on surface-tethered CAPs and Nylon3 in displaying their genuine functions: an appropriate medium-length antifouling PEG layer, OEG8, enables favorable cell adhesion and displaying the genuine function of cell adhesive molecules; a short OEG4 antifouling layer is associated with overestimated cell adhesion due to unwanted fouling; a long PEG2K antifouling layer results in underestimated cell adhesion due to low surface density of polypeptide that is caused by the substantially lower density of reactive sites on PEG2K-modified surfaces at 0.7 chain/nm^2 relative to OEG4- and OEG8-modified surfaces at 1.4 and 1.2 chain/nm^2, respectively (Figure 1b) and possible embedding of reactive sites by the long PEG2K chains. We discontinued exploring PEG2K as the antifouling layer in the following studies because a poor cell adhesion is obtained generally using this long-chain PEG as the antifouling layer for further surfaces modified with CAPs.

Cell Migration Modulated by PEG. In addition to cell adhesion, cell migration is another parameter that can be used to evaluate cellular interactions with CAP-modified surfaces.[32] EC and SMC are a pair of extensively studied cell types for vascular-related studies and applications, with selective EC adhesion and migration highly desired.[33,34] The laminin-derived YIGSR peptide is well recognized and extensively used for its selectivity on EC.[35] When using TCPS without an antifouling layer, ECs migrated much slower and traveled significantly shorter distances than did SMCs; when an OEG4-covered surface was modified with YIGSR (OEG4-YIGSR), the result unfortunately is identical to TCPS although with a

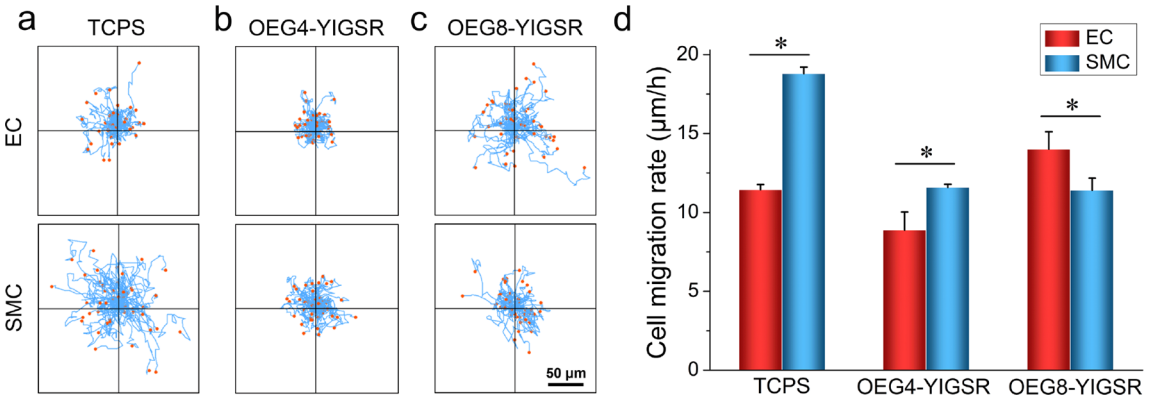

Figure 5. EC and SMC migration on YIGSR-modified surfaces indicate OEG8 as an excellent antifouling layer to demonstrate the genuine and optimal function of EC-selective YIGSR peptide. (a–c) Migration traces of ECs and SMCs on the TCPS surface, YIGSR-modified OEG4 surface, and YIGSR-modified OEG8 surface, respectively. Cells were continuously tracked every 15 min for 12 h. Scale bar: 50 μm. (d) Quantitative analysis of cell migration rate in panels (a), (b), and (c). All data are presented as means ± SD. Statistical analysis was conducted using one-way ANOVA and Tukey's post-test. (*) $p < 0.05$.

DOI: 10.1021/jacs.9b07105
J. Am. Chem. Soc. XXXX, XXX, XXX−XXX

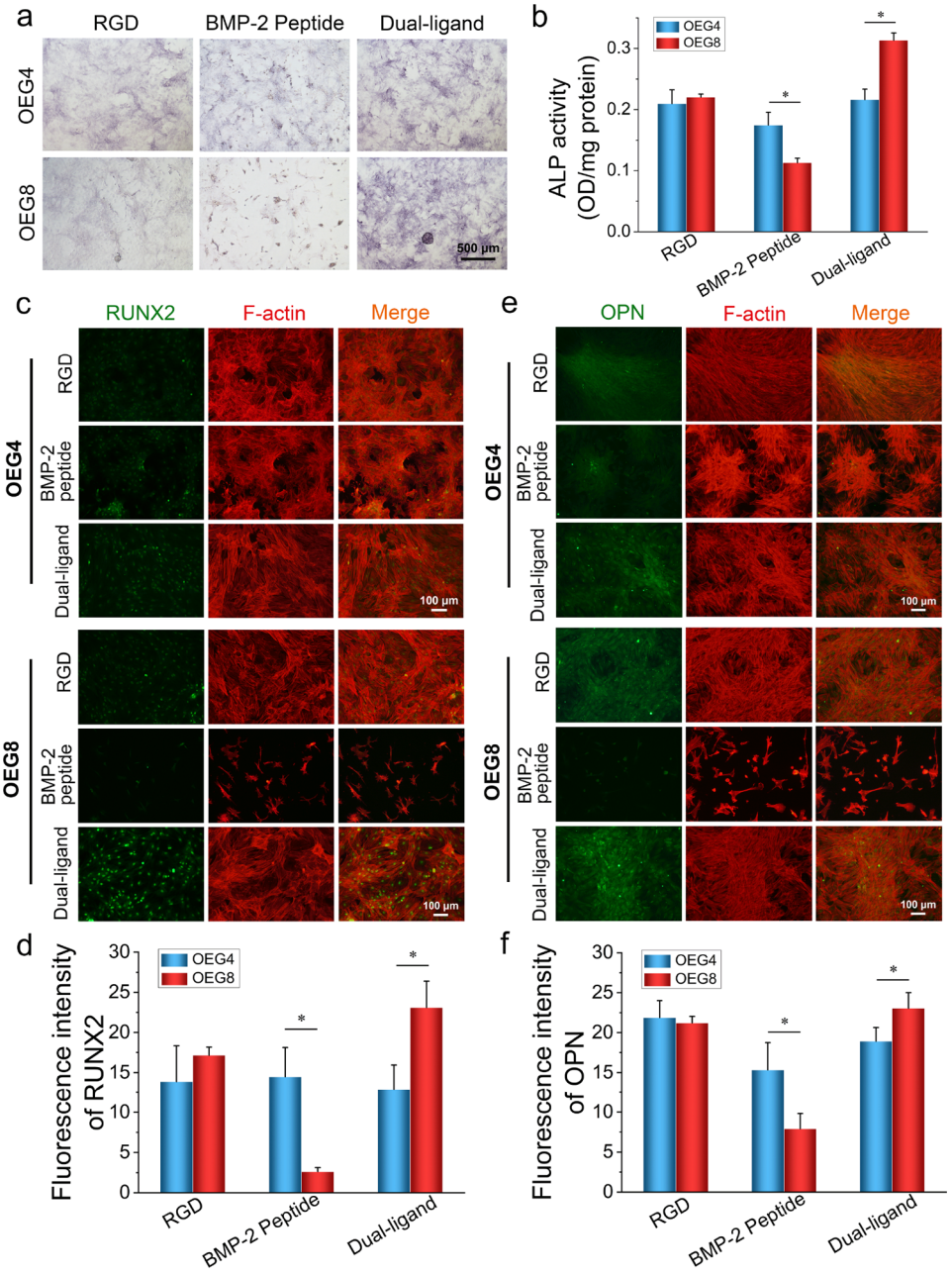

Figure 6. BMSC differentiation on RGD peptide-, BMP-2 peptide-, and RGD/BMP-2 dual ligand-modified surfaces indicates OEG8 as an excellent antifouling layer to demonstrate the genuine and optimal function of BMP-2 peptide in modulating stem cell differentiation. (a, b) ALP staining and quantitative analysis of cells at day 7 post cell seeding on various surfaces. n = 5 for each type of surface. (c, d) Representative immunofluorescent micrographs and RUNX2 quantification of BMSCs on various surfaces at day 7 post cell seeding. Green = RUNX2, red = actin; scale bar, 100 μm. n = 5 for each group. (e, f) Representative immunofluorescent micrographs and OPN quantification of BMSCs on various surfaces at day 21 post cell seeding. Green = OPN, red = actin; scale bar, 100 μm. n = 5 for each group. All data are presented as means ± SD. Statistical analysis was conducted using one-way ANOVA and Tukey's post-test. (*) $p < 0.05$.

substantially reduced SMC migration rate and migration distance (Figure 5a–c). In both cases, surface fouling leads to the observed SMC-preferred cell migration that is opposite to expected EC selectivity of the YIGSR peptide. When an OEG8-covered surface was modified with YIGSR (OEG8-YIGSR), ECs migrated much faster and traveled significantly longer distances than did SMCs, a result matching the expected EC selectivity of the YIGSR peptide. It is noteworthy that the migration rate of ECs at 14 μm/h on the OEG8-YIGSR surface was significantly faster than that at 11.4 and 8.9 μm/h on the TCPS surface and OEG4-YIGSR surface, respectively (Figure 5d). The favorable result from OEG8-YIGSR is attributed to the combination of effective antifouling and a high enough density of YIGSR on the surface to fully display the genuine function of the EC-selective YIGSR peptide, including EC-selective cell adhesion and polarization for cell migration.

Stem Cell Differentiation on Dual-Ligand Surface. More sophisticated stem cell differentiation is also closely regulated by functional peptides especially using dual ligands, such as the combination of RGD peptide and BMP-2 peptide, to synergistically enhance the differentiation of bone marrow mesenchymal stem cells (BMSCs) into osteoblasts.[36,37] We first

DOI: 10.1021/jacs.9b07105
J. Am. Chem. Soc. XXXX, XXX, XXX−XXX

evaluated the osteogenesis at an early time point by monitoring the ALP activity of BMSCs and the production of mineralized matrix after BMSCs were cultured on functional peptides-modified surfaces for 7 days. We observed no significant difference in ALP activity between BMSCs on OEG4-RGD and OEG8-RGD surfaces, which agrees with RGD's function to promote cell adhesion but not cell differentiation at an early stage (Figure 6a,b). The BMP-2 peptide can promote osteogenic differentiation of BMSCs, but weakly supports cell adhesion. Therefore, it is not surprising to see a weaker ALP activity of BMSCs on the OEG8-BMP-2 peptide surface compared to that on the OEG4-BMP-2 peptide surface because the latter is overestimated by the increased cell adhesion due to nonspecific fouling (Figure 6a,b). When RGD peptide was used in combination with BMP-2 peptide to increase cell adhesion, this dual-ligand system substantially enhanced (almost 3-fold increase compared to the OEG8-BMP-2 peptide) the ALP activity of BMSCs on OEG8-dual-ligand surface, which is significantly better than that on OEG4-dual-ligand surface because the function of the BMP-2 peptide was diminished by the OEG4-associated fouling (Figure 6a,b). We evaluated the amount of RUNX2 within cells as an early marker of osteogenic differentiation. Both staining and quantitative analysis indicated that the dual-ligand surface enables the optimal performance of cell differentiation when OEG8 was used as the antifouling layer (Figure 6c,d). We also evaluated a prolonged culture of BMSCs on day 21 using the osteopontin (OPN) marker, which is a structural protein synthesized by osteoblasts and osteocytes and is considered an important factor in bone remodeling. The dual-ligand surface using OEG8 as antifouling layer demonstrated better performance than that using OEG4 as antifouling layer, in controlled cell differentiation with the presence of discrete areas of intense cell aggregation, early nodule formation, and OPN-positive regions (Figure 6e,f).

DISCUSSION

CAPs and other functional peptides are extensively studied and utilized in tissue engineering scaffolds and biomedical devices to facilitate cell adhesion, proliferation, migration, and differentiation with or without use of an antifouling layer. PEG is a type of easily accessible and widely used antifouling molecule. Nevertheless, the impact of the PEG antifouling layer on the performance of functional peptides is still ambiguous, and it is generally considered to work as long as a PEG antifouling layer is used or a long PEG is used to ensure an excellent antifouling property.[23] Our study hereby demonstrates that an appropriate PEG molecule is critical to fully and correctly display the genuine function of CAPs and other functional peptides. Although PEG2K provides an excellent antifouling property easily, our studies indicate that long-chain PEG can substantially and even almost completely diminish the function of CAPs and other functional peptides because the collapsed and long, bulky PEG chains as random coils result in a low density of reactive sites for functional molecule grafting and therefore a low density of functional peptides on the surface. Unfortunately, the performance of most CAPs and functional peptides is ligand density dependent. Surprisingly, when a short PEG, such as OEG4, is used as the antifouling fragment, we observed nonspecific cell adhesion, substantially diminished cell type specific adhesion, the opposite result of cell migration, and nonoptimal control of cell differentiation. The medium-length OEG8 is optimal by providing efficient antifouling and presenting functional peptides with high density on the surface to control cell adhesion, migration, and differentiation. In short, this study reveals the importance of choosing appropriate PEG molecules as the antifouling layer for the study and application of CAPs and other functional peptides. Our study provides a general guideline in selecting optimal PEG molecules for the identification, study, and application of CAPs and other functional peptides, which helps to avoid confusing and even controversial results and fully display the genuine function of CAPs and other functional peptides.

ASSOCIATED CONTENT

Supporting Information

The Supporting Information is available free of charge on the ACS Publications website at DOI: 10.1021/jacs.9b07105.

Protein adsorption, SPR sensorgram, GPC characterization, NMR analysis (PDF)

AUTHOR INFORMATION

Corresponding Author

*rliu@ecust.edu.cn

ORCID

Qi Chen: 0000-0002-5982-9249
Donghui Zhang: 0000-0002-8934-8550
Wenjing Zhang: 0000-0002-6076-8017
Haodong Zhang: 0000-0002-1186-8732
Jingcheng Zou: 0000-0002-4839-9650
Zhengwei Mao: 0000-0001-7990-2856
Yuan Yuan: 0000-0001-7877-3175
Changyou Gao: 0000-0001-5084-7208
Runhui Liu: 0000-0002-7699-086X

Notes

The authors declare the following competing financial interest(s): R.L. and Q.C. are co-inventors on a patent covering surface functional modification with an antifouling PEG layer.

ACKNOWLEDGMENTS

We thank Dr. T. Wei, Dr. Q. Yu, and Dr. H. Chen at Soochow University for assistance in ellipsometry characterization. We also appreciate the Research Center of Analysis and Test of East China University of Science and Technology for the help with the characterization. This research was supported by the National Key Research and Development Program of China (2016YFC1100401), the National Natural Science Foundation of China (No. 21774031), the National Natural Science Foundation of China for Innovative Research Groups (No. 51621002), the "Eastern Scholar Professorship" from Shanghai local government (TP2014034), the Natural Science Foundation of Shanghai (18ZR1410300), the National Special Fund for State Key Laboratory of Bioreactor Engineering (2060204), and the Fundamental Research Funds for the Central Universities (22221818014).

REFERENCES

(1) Huang, G.; Li, F.; Zhao, X.; Ma, Y.; Li, Y.; Lin, M.; Jin, G.; Lu, T. J.; Genin, G. M.; Xu, F. Functional and Biomimetic Materials for Engineering of the Three-Dimensional Cell Microenvironment. *Chem. Rev.* **2017**, *117* (20), 12764−12850.

(2) Pierschbacher, M. D.; Ruoslahti, E. Cell attachment activity of fibronectin can be duplicated by small synthetic fragments of the molecule. *Nature* **1984**, *309* (5963), 30−33.

DOI: 10.1021/jacs.9b07105
J. Am. Chem. Soc. XXXX, XXX, XXX−XXX

(3) Hasenbein, M. E.; Andersen, T. T.; Bizios, R. Micropatterned surfaces modified with select peptides promote exclusive interactions with osteoblasts. *Biomaterials* **2002**, *23* (19), 3937−3942.
(4) Massia, S. P.; Rao, S. S.; Hubbell, J. A. Covalently immobilized laminin peptide Tyr-Ile-Gly-Ser-Arg (YIGSR) supports cell spreading and co-localization of the 67-kilodalton laminin receptor with alpha-actinin and vinculin. *J. Biol. Chem.* **1993**, *268* (11), 8053−8059.
(5) Gobin, A. S.; West, J. L. Val-ala-pro-gly, an elastin-derived non-integrin ligand: Smooth muscle cell adhesion and specificity. *J. Biomed. Mater. Res.* **2003**, *67A* (1), 255−259.
(6) Saito, A.; Suzuki, Y.; Ogata, S.-i.; Ohtsuki, C.; Tanihara, M. Activation of osteo-progenitor cells by a novel synthetic peptide derived from the bone morphogenetic protein-2 knuckle epitope. *Biochim. Biophys. Acta, Proteins Proteomics* **2003**, *1651* (1−2), 60−67.
(7) Hussey, G. S.; Dziki, J. L.; Badylak, S. F. Extracellular matrix-based materials for regenerative medicine. *Nat. Rev. Mater.* **2018**, *3* (7), 159−173.
(8) Murphy, W. L.; McDevitt, T. C.; Engler, A. J. Materials as stem cell regulators. *Nat. Mater.* **2014**, *13* (6), 547−557.
(9) Zhang, H.; Zheng, X.; Ahmed, W.; Yao, Y.; Bai, J.; Chen, Y.; Gao, C. Design and Applications of Cell-Selective Surfaces and Interfaces. *Biomacromolecules* **2018**, *19* (6), 1746−1763.
(10) Chen, L.; Yan, C.; Zheng, Z. Functional polymer surfaces for controlling cell behaviors. *Mater. Today* **2018**, *21* (1), 38−59.
(11) Chang, B.; Zhang, M.; Qing, G.; Sun, T. Dynamic biointerfaces: from recognition to function. *Small* **2015**, *11* (9−10), 1097−1112.
(12) Raphel, J.; Karlsson, J.; Galli, S.; Wennerberg, A.; Lindsay, C.; Haugh, M. G.; Pajarinen, J.; Goodman, S. B.; Jimbo, R.; Andersson, M.; Heilshorn, S. C. Engineered protein coatings to improve the osseointegration of dental and orthopaedic implants. *Biomaterials* **2016**, *83*, 269−282.
(13) Lee, M.-R.; Stahl, S. S.; Gellman, S. H.; Masters, K. S. Nylon-3 Copolymers that Generate Cell-Adhesive Surfaces Identified by Library Screening. *J. Am. Chem. Soc.* **2009**, *131* (46), 16779−16789.
(14) von der Mark, K.; Park, J. Engineering biocompatible implant surfaces. *Prog. Mater. Sci.* **2013**, *58* (3), 327−381.
(15) Jin, S.; Yao, H. T.; Weber, J. L.; Melkoumian, Z. K.; Ye, K. M. A Synthetic, Xeno-Free Peptide Surface for Expansion and Directed Differentiation of Human Induced Pluripotent Stem Cells. *PLoS One* **2012**, *7* (11), e50880.
(16) Huettner, N.; Dargaville, T. R.; Forget, A. Discovering Cell-Adhesion Peptides in Tissue Engineering: Beyond RGD. *Trends Biotechnol.* **2018**, *36* (4), 372−383.
(17) Wei, Q.; Becherer, T.; Angioletti-Uberti, S.; Dzubiella, J.; Wischke, C.; Neffe, A. T.; Lendlein, A.; Ballauff, M.; Haag, R. Protein interactions with polymer coatings and biomaterials. *Angew. Chem., Int. Ed.* **2014**, *53* (31), 8004−8031.
(18) Yu, Q.; Zhang, Y.; Wang, H.; Brash, J.; Chen, H. Anti-fouling bioactive surfaces. *Acta Biomater.* **2011**, *7* (4), 1550−1557.
(19) Kadem, L. F.; Holz, M.; Suana, K. G.; Li, Q.; Lamprecht, C.; Herges, R.; Selhuber-Unkel, C. Rapid Reversible Photoswitching of Integrin-Mediated Adhesion at the Single-Cell Level. *Adv. Mater.* **2016**, *28* (9), 1799−1802.
(20) Jiang, S.; Cao, Z. Ultralow-fouling, functionalizable, and hydrolyzable zwitterionic materials and their derivatives for biological applications. *Adv. Mater.* **2010**, *22* (9), 920−932.
(21) Ye, K.; Wang, X.; Cao, L.; Li, S.; Li, Z.; Yu, L.; Ding, J. Matrix Stiffness and Nanoscale Spatial Organization of Cell-Adhesive Ligands Direct Stem Cell Fate. *Nano Lett.* **2015**, *15* (7), 4720−4729.
(22) Celiz, A. D.; Smith, J. G.; Patel, A. K.; Hook, A. L.; Rajamohan, D.; George, V. T.; Flatt, L.; Patel, M. J.; Epa, V. C.; Singh, T.; Langer, R.; Anderson, D. G.; Allen, N. D.; Hay, D. C.; Winkler, D. A.; Barrett, D. A.; Davies, M. C.; Young, L. E.; Denning, C.; Alexander, M. R. Discovery of a Novel Polymer for Human Pluripotent Stem Cell Expansion and Multilineage Differentiation. *Adv. Mater.* **2015**, *27* (27), 4006−4012.
(23) Roberts, J. N.; Sahoo, J. K.; McNamara, L. E.; Burgess, K. V.; Yang, J.; Alakpa, E. V.; Anderson, H. J.; Hay, J.; Turner, L. A.; Yarwood, S. J.; Zelzer, M.; Oreffo, R. O.; Ulijn, R. V.; Dalby, M. J. Dynamic Surfaces for the Study of Mesenchymal Stem Cell Growth through Adhesion Regulation. *ACS Nano* **2016**, *10* (7), 6667−6679.
(24) Benoit, D. S.; Anseth, K. S. The effect on osteoblast function of colocalized RGD and PHSRN epitopes on PEG surfaces. *Biomaterials* **2005**, *26* (25), 5209−5220.
(25) Lu, X.; Nicovich, P. R.; Zhao, M.; Nieves, D. J.; Mollazade, M.; Vivekchand, S. R. C.; Gaus, K.; Gooding, J. J. Monolayer surface chemistry enables 2-colour single molecule localisation microscopy of adhesive ligands and adhesion proteins. *Nat. Commun.* **2018**, *9*, 3320.
(26) Noel, S.; Hachem, A.; Merhi, Y.; De Crescenzo, G. Development of a Polyester Coating Combining Antithrombogenic and Cell Adhesive Properties: Influence of Sequence and Surface Density of Adhesion Peptides. *Biomacromolecules* **2015**, *16* (6), 1682−1694.
(27) Wei, Y.; Ji, Y.; Xiao, L.; Lin, Q.; Ji, J. Different complex surfaces of polyethyleneglycol (PEG) and REDV ligand to enhance the endothelial cells selectivity over smooth muscle cells. *Colloids Surf., B* **2011**, *84* (2), 369−378.
(28) Li, D.; Chen, H.; Glenn McClung, W.; Brash, J. L. Lysine-PEG-modified polyurethane as a fibrinolytic surface: Effect of PEG chain length on protein interactions, platelet interactions and clot lysis. *Acta Biomater.* **2009**, *5* (6), 1864−1871.
(29) Qian, Y.; Qi, F.; Chen, Q.; Zhang, Q.; Qiao, Z.; Zhang, S.; Wei, T.; Yu, Q.; Yu, S.; Mao, Z.; Gao, C.; Ding, Y.; Cheng, Y.; Jin, C.; Xie, H.; Liu, R. Surface Modified with a Host Defense Peptide-Mimicking beta-Peptide Polymer Kills Bacteria on Contact with High Efficacy. *ACS Appl. Mater. Interfaces* **2018**, *10*, 15395−15400.
(30) Xia, Y.; Adibnia, V.; Huang, R.; Murschel, F.; Faivre, J.; Xie, G.; Olszewski, M.; De Crescenzo, G.; Qi, W.; He, Z.; Su, R.; Matyjaszewski, K.; Banquy, X. Biomimetic Bottlebrush Polymer Coatings for Fabrication of Ultralow Fouling Surfaces. *Angew. Chem., Int. Ed.* **2019**, *58* (5), 1308−1314.
(31) Liu, R.; Masters, K. S.; Gellman, S. H. Polymer chain length effects on fibroblast attachment on nylon-3-modified surfaces. *Biomacromolecules* **2012**, *13* (4), 1100−1105.
(32) Yu, S.; Gao, Y.; Mei, X.; Ren, T.; Liang, S.; Mao, Z.; Gao, C. Preparation of an Arg-Glu-Asp-Val Peptide Density Gradient on Hyaluronic Acid-Coated Poly(epsilon-caprolactone) Film and Its Influence on the Selective Adhesion and Directional Migration of Endothelial Cells. *ACS Appl. Mater. Interfaces* **2016**, *8* (43), 29280−29288.
(33) Yang, Z.; Xiong, K.; Qi, P.; Yang, Y.; Tu, Q.; Wang, J.; Huang, N. Gallic acid tailoring surface functionalities of plasma-polymerized allylamine-coated 316L SS to selectively direct vascular endothelial and smooth muscle cell fate for enhanced endothelialization. *ACS Appl. Mater. Interfaces* **2014**, *6* (4), 2647−2656.
(34) Ding, X.; Chin, W.; Lee, C. N.; Hedrick, J. L.; Yang, Y. Y. Peptide-Functionalized Polyurethane Coatings Prepared via Grafting-To Strategy to Selectively Promote Endothelialization. *Adv. Healthcare Mater.* **2018**, *7* (5), 170094.
(35) Maeda, T.; Titani, K.; Sekiguchi, K. Cell-adhesive activity and receptor-binding specificity of the laminin-derived YIGSR sequence grafted onto Staphylococcal protein A. *J. Biochem.* **1994**, *115* (2), 182−189.
(36) Freeman, R.; Stephanopoulos, N.; Alvarez, Z.; Lewis, J. A.; Sur, S.; Serrano, C. M.; Boekhoven, J.; Lee, S. S.; Stupp, S. I. Instructing cells with programmable peptide DNA hybrids. *Nat. Commun.* **2017**, *8*, 15982.
(37) Ma, Y.; Policastro, G. M.; Li, Q.; Zheng, J.; Jacquet, R.; Landis, W. J.; Becker, M. L. Concentration-Dependent hMSC Differentiation on Orthogonal Concentration Gradients of GRGDS and BMP-2 Peptides. *Biomacromolecules* **2016**, *17* (4), 1486−1495.

DOI: 10.1021/jacs.9b07105
J. Am. Chem. Soc. XXXX, XXX, XXX−XXX